



## Factors controlling variability in nearshore fecal pollution: The effects of mortality

M.A. Rippy<sup>a,\*</sup>, P.J.S. Franks<sup>a</sup>, F. Feddersen<sup>a</sup>, R.T. Guza<sup>a</sup>, D.F. Moore<sup>b,1</sup>

<sup>a</sup> Scripps Institution of Oceanography, La Jolla, CA 92093-0218, USA

<sup>b</sup> Orange County Public Health Laboratory, Santa Ana, CA 92706, USA

### ARTICLE INFO

#### Keywords:

Fecal indicator bacteria  
Mortality  
Advection  
Diffusion  
Surfzone

### ABSTRACT

A suite of physical–biological models was used to explore the importance of mortality and fluid dynamics in controlling concentrations of fecal indicator bacteria (FIB) at Huntington Beach, CA. An advection–diffusion (AD) model provided a baseline to assess improvements in model skill with the inclusion of mortality. Six forms of mortality were modeled. All mortality models performed better than the AD model, especially at offshore sampling stations, where model skill increased from <0.18 to >0.50 (*Escherichia coli*) or <−0.14 to >0.30 (*Enterococcus*). Models including cross-shore variable mortality rates reproduced FIB decay accurately ( $p < 0.05$ ) at more stations than models without. This finding is consistent with analyses that revealed cross-shore variability in *Enterococcus* species composition and solar dose response. No best model was identified for *Enterococcus*, as all models including cross-shore variable mortality performed similarly. The best model for *E. coli* included solar-dependent and cross-shore variable mortality.

© 2012 Elsevier Ltd. All rights reserved.

### 1. Introduction

Human pathogenic bacteria are a persistent social, health, and economic problem at beaches around the world. The significant health risks and economic losses associated with beach bacterial pollution have prompted extensive monitoring programs and concerted research efforts aimed at predicting pollution events (Boehm, 2003; Boehm et al., 2005; Sanders et al., 2005).

Multiple mechanisms have been identified that introduce pathogens and associated fecal indicator bacteria (FIB) into the surfzone, including: tidal pumping from estuaries (Grant et al., 2001) and groundwater (Boehm et al., 2004), river flow (Gersberg et al., 2006), and re-suspension from sediments (Yamahara et al., 2007). Similarly, many factors governing rates of FIB mortality in seawater have been identified, including: solar insolation (Sinton et al., 2002, 2007), temperature (Solic and Krstulovic, 1992), dissolved organic nutrients (Hartke et al., 1998), dissolved oxygen (Curtis et al., 1992), and protistan grazing (Hartke et al., 2002). What is often absent from efforts to understand nearshore FIB persistence, however, are syntheses of physical and biological dynamics. Only a handful of studies have attempted to quantify the importance of different physical or biological processes in controlling the extent and intensity of FIB pollution in the surfzone (Boehm et al., 2005, 2009; Grant et al., 2001). Even fewer use models as vehicles to test hypotheses concerning the accuracy with

which different combinations of mechanisms can reproduce actual FIB data (Boehm, 2003; Boehm et al. 2005; Sanders et al., 2005). Here, we present a study designed specifically for this purpose.

Data were acquired during a 5-h field program at Huntington Beach, CA, on October 16th, 2006, that monitored nearshore FIB concentrations, waves, and currents. In this manuscript we explore the role of biological dynamics (in this case mortality) in controlling the spatial and temporal variability of FIB at Huntington Beach. Six different mortality functions representing different FIB mortality mechanisms are added to an individual based model of FIB that contains alongshore advection and cross-shore variable horizontal diffusion (the AD model). These new mortality models, together with additional data (*Enterococcus* species distribution and time dependent solar insolation dose observations), are used to evaluate hypotheses regarding FIB mortality mechanisms in the nearshore.

The mortality mechanisms explored in this paper are: spatially and temporally constant mortality (null hypothesis), spatially constant solar-induced mortality, stationary cross-shore mortality gradients, FIB source-dependent mortality, and two combinations of the above. Solar-induced mortality was explored because insolation is often posited as a dominant source of mortality for nearshore FIB, and has been suggested to affect FIB at Huntington Beach (Boehm et al., 2002; Sinton et al., 2002). Cross-shore mortality gradients were examined because surfzone and offshore waters often have different dynamics, which can result in cross-shore gradients of properties affecting FIB mortality, like temperature, grazers and turbidity (Omand et al., 2011; Reniers et al., 2009; Smith and Largier, 1995). Turbidity gradients, in particular, can affect the penetration of solar insolation, which, if FIB are solar sensitive,

\* Corresponding author. Tel.: +1 831 419 5285.

E-mail address: [mrippy@ucsd.edu](mailto:mrippy@ucsd.edu) (M.A. Rippy).

<sup>1</sup> Present address: PO Box 239, Kalaheo, HI 96741, USA.

may result in cross-shore variable FIB mortality gradients that the organisms move through as they are advected and diffused across shore (Alkan et al., 1995; Whitman et al., 2004). One of our two combination mortality functions includes both cross-shore mortality gradients and solar sensitivity to depict this particular mortality mechanism. Lastly, source-specific FIB mortality was examined because FIB from different sources can have different mortality rates (Sinton et al., 2002), and multiple FIB sources have been identified at Huntington Beach (Boehm et al., 2004; Grant et al., 2001; Rippy et al., in press).

## 2. Methods

### 2.1. Sampling design

Details of the HB06 FIB experiment are reported in Rippy et al. (in press). Briefly, FIB concentrations at Huntington Beach (which runs approximately north–south) were measured for 5 h on October 16th, 2006, at eight stations. Four of these stations spanned a 1000 m alongshore transect from the Santa Ana River, north. The remaining four stations were on a 300 m cross-shore transect starting at the northernmost alongshore station and terminating at an offshore mooring (Rippy et al., in press, their Fig. 1). Water samples (100 ml) were collected at all stations, every 20 min, from 0650 to 1150 PDT. All samples were analyzed for *Escherichia coli* (IDEXX Colilert) and *Enterococcus* (USEPA method 1600) concentrations by Orange County Sanitation District personnel.

Acoustic Doppler Velocimeters (ADV's) mounted on fixed tripod frames were used to measure currents along the shoreward-most 150 m of the cross-shore transect (Rippy et al., in press, their Fig. 1). These data were used to force alongshore currents in the 2D FIB models discussed below.

### 2.2. *Enterococcus* species identification

*Enterococcus* species identification was performed to detect spatial patterns that could indicate the presence of multiple *Enterococcus* sources (potentially exhibiting differing mortality rates) in the nearshore. Species were identified at the Orange County Public Health Laboratory using presumptive *Enterococcus* colonies grown up from water samples on mEI agar plates. Three presumptive *Enterococcus* colonies were examined per plate when colony counts allowed, corresponding to three colonies per water sample. Initial colony identification was performed using a Microscan Walk-Away 96 system containing Microscan Pos Combo Type 12 panels (Dade Bering Inc., West Sacramento, CA). The type 12 panel contains 27 dried biochemical tests for the identification of gram-positive bacteria. The software database for this system contains 42 gram-positive cocci, including seven species of *Enterococcus*. Additional biochemical tests were also used for identification purposes including carbohydrate fermentation in brain heart infusion broth with 1% sucrose (35 °C), a motility test using motility medium with Triphenyl Tetrazolium Chloride (30 °C), and a pigment production assay using Trypticase soy agar with 5% sheep's blood (35 °C). Final identification was determined utilizing published standard biochemical identification charts (Moore et al., 2008).

Due to the retentive nature of the surfzone (Reniers et al., 2009), special attention was paid to cross-shore variability of *Enterococcus* species distributions. All identified *Enterococcus* isolates were classified based on their collection location as either “onshore” (SAR, TM, FHM, and F1) or “offshore” (stations  $\geq 50$  m seaward of the surfzone: F5 and F7). Species composition onshore vs. offshore was compared using a Pearson chi-squared test.

### 2.3. Solar insolation studies

Solar insolation data were collected using a Davis Vantage Pro Plus cosine pyranometer stationed 3.2 km inland of Huntington Beach, with a sampling frequency of once per minute (SI Fig. 1). This sensor was part of a weather station managed by the Golden West College Observatory. Solar radiation dosages were calculated by integrating solar insolation over the 20-min FIB sampling interval. All statistical analyses were performed using MATLAB (Mathworks, Natick, MA).

To assess the role of solar insolation as a factor controlling temporal decay in FIB concentrations at Huntington Beach, decay rates were calculated for both *Enterococcus* and *E. coli* at each sampling station and compared to solar insolation dose. FIB decay rates were calculated as  $r = \log[N(t)/N(t - \Delta t)]/(\Delta t)$ , where  $r$  is the FIB-specific decay rate,  $N(t)$  is population at time  $t$ , and the time interval  $\Delta t$  is 20 min, the FIB sampling interval. Note that these decay rates include all processes leading to local losses of FIB, including advection, diffusion and mortality. Here, the term *decay rate* will always refer to total change in FIB concentration (from data or model outputs) with time, regardless of the processes forcing those changes. In contrast, the term *mortality rate* will be used to denote the portion of FIB decay that is due to FIB senescence alone, and not caused by advection or diffusion.

Solar penetration may be significantly reduced in the surfzone due to turbidity and bubbles (Alkan et al., 1995; Smith and Largier, 1995). To determine whether or not the relationship between solar dose and FIB decay differed in the surfzone vs. farther offshore, FIB sampling stations were divided into “onshore” and “offshore” locations (see *Enterococcus* species identification above). The solar dose/decay rate data for these sets of stations were pooled, and a regression line was fit to each set to determine onshore- and offshore solar dose-FIB decay rate relationships.

### 2.4. 2D individual based FIB models

#### 2.4.1. Model structure: AD

Rippy et al. (in press) constructed a 2D ( $x$  = alongshore,  $y$  = cross-shore) individual-based FIB model (AD) and parameterized it based on literature values, HB06 physical measurements, and model fits to HB06 FIB data (*E. coli* and *Enterococcus*). The AD model includes alongshore advection,  $u(y,t)$ , given by the cross-shore transect of ADV's mentioned above, and horizontal diffusion ( $\kappa_h$ ), acting both along- and across-shore. Advection and horizontal diffusion were assumed to be uniform alongshore. The local magnitude of horizontal diffusion was defined as,

$$\kappa_h = \kappa_0 + \frac{(\kappa_1 - \kappa_0)}{2} \left\{ 1 - \tanh \left[ \frac{y - y_0}{y_{scale}} \right] \right\} \quad (1)$$

where  $\kappa_0$  is the background (offshore) diffusivity,  $\kappa_1$  is the elevated surfzone diffusivity,  $y_0$  is the cross-shore midpoint of the transition between  $\kappa_0$  and  $\kappa_1$  (i.e., the offshore edge of the surfzone) and  $y_{scale}$  determines the width of this transition in the cross-shore. The  $\kappa_0$ ,  $\kappa_1$ ,  $y_0$ , and  $y_{scale}$  values used here are those that provided the best AD model fits to Huntington Beach FIB data:  $0.05 \text{ m}^2 \text{ s}^{-1}$ ,  $0.5 \text{ m}^2 \text{ s}^{-1}$ , 50 m and 5 m, respectively (Rippy et al., in press). The fit metric used to assess this, and all other model-data fits presented in this paper, was model skill (Krause et al., 2005):

$$\text{Skill} = 1 - \frac{\text{mean}(C_{obs} - C_{mod})^2}{\text{mean}(C_{obs} - \bar{C}_{obs})^2} \quad (2)$$

Here,  $C_{obs}$  is log observed FIB concentration,  $C_{mod}$  is log modeled FIB concentration, and  $\bar{C}_{obs}$  is the mean of  $\log(C_{obs})$  over all stations and times. Skill represents the degree to which variability in the data is better explained by the model than by the global space–time mean

of the data. Depending on context, skill was calculated for individual stations, groups of stations, or all stations together, by changing the numerator of Eq. (2).

#### 2.4.2. Model initialization

For all model formulations, 80,000 bacterial particles containing a concentration of FIB ( $C$ ) were initialized in a uniform grid extending 160 m offshore, and from the Santa Ana River to 600 m north of F1 (the northernmost sampling frame) in the alongshore. These along- and across-shore boundaries for the initial FIB patch were determined to produce the best fits between FIB data and the AD model (Rippy et al., in press).

#### 2.4.3. Model structure: mortality models

All mortality models were of the form

$$\frac{dC}{dt} = -MC \quad (3)$$

where  $C$  is FIB concentration and  $M$  is a FIB mortality function. In the AD model,  $M$  was set to zero, and the concentration of FIB in each initial particle was fixed.  $M$  was non-zero for all mortality models. Eq. (3) was solved numerically using the Euler finite-difference method. Six different functional forms of  $M$  were examined, two of which (ADC and ADI) contain only one mortality parameter ( $m$ ). The remaining four (ADS, ADG, ADSI, and ADGI) contain two mortality parameters each ( $m_0$  and  $m_1$ ), allowing FIB mortality to vary across shore.

#### 2.4.4. One parameter mortality models: ADC and ADI

In the one-parameter models FIB mortality was set either to a constant rate  $m$  (units:  $s^{-1}$ ) (ADC model) or a time-dependent rate determined by measured solar insolation  $I(t)$  scaled by maximum solar insolation  $I_{max}$  (ADI model):

$$\text{ADC model: } M = m \quad (4)$$

$$\text{ADI model: } M = \frac{mI(t)}{I_{max}} \quad (5)$$

Appropriate test ranges for the mortality parameters were selected from literature (Boehm et al., 2005; Sinton et al., 2002; Troussellier et al., 1998). Final parameter values for both models, and those described below, were those that maximized the skill between modeled and observed FIB concentrations (*E. coli* and *Enterococcus*).

#### 2.4.5. Two-parameter mortality models: source-specific

In all source-specific mortality models, particles initialized 0–50 m cross-shore were considered “onshore” particles and those initialized 50–160 m cross-shore were considered “offshore” particles. Particle mortality was set according to the particle’s initial onshore or offshore location (its “source”) and was either constant (onshore =  $m_0$  and offshore =  $m_1$ ) (ADS model), or dependent on scaled solar insolation (ADSI model):

ADS model:

$$M = \begin{cases} m_0 & \text{Initial Particle Location} < 50 \text{ m Cross-shore} \\ m_1 & \text{Initial Particle Location} > 50 \text{ m Cross-shore} \end{cases} \quad (6)$$

ADSI model:

$$M = \begin{cases} \frac{m_0 I(t)}{I_{max}} & \text{Initial Particle Location} < 50 \text{ m Cross-shore} \\ \frac{m_1 I(t)}{I_{max}} & \text{Initial Particle Location} > 50 \text{ m Cross-shore} \end{cases} \quad (7)$$

Note that in the ADS and ADSI models, mortality rate is an intrinsic property of each particle, and tracks individual particles in a Lagrangian manner.

#### 2.4.6. Two-parameter mortality models: cross-shore mortality gradient

In all cross-shore gradient-dependent mortality models the mortality function  $M$  was determined either by the cross-shore location of the particle (ADG), or by the cross-shore location of the particle and scaled solar insolation (ADGI). The cross-shore dependence of  $M$  was similar to the horizontal diffusion function used in all models (Eq. (1)):

ADG model:

$$M = m_1 + \left( \frac{m_0 - m_1}{2} \right) \left[ 1 - \tanh \left( \frac{y - y_0}{y_{scale}} \right) \right] \quad (8)$$

ADGI model:

$$M = \frac{I(t)}{I_{max}} \left\{ m_1 + \left( \frac{m_0 - m_1}{2} \right) \left[ 1 - \tanh \left( \frac{y - y_0}{y_{scale}} \right) \right] \right\} \quad (9)$$

where  $m_0$  is surfzone mortality,  $m_1$  is offshore mortality,  $y_0$  is the offshore edge of the surfzone, and  $y_{scale}$  determines the cross-shore scale of the surfzone/offshore transition. Values for  $y_0$  and  $y_{scale}$  were 50 m and 5 m, respectively, the same values used to parameterize diffusivity (Eq. (1)). Note that in the ADG and ADGI models, mortality is not an intrinsic property of a given particle (as in the ADS and ADSI models). Instead, particles move through stationary cross-shore mortality gradients and take on different mortality rates based on their cross-shore location within those gradients.

### 3. Results/discussion

#### 3.1. Spatial patterns in *Enterococcus* species distribution

All presumptive *Enterococcus* isolates were found to come from one of nine different groups. Five of these groups were common fecal (*E. faecalis*, *E. faecium*, *E. hirae*) and plant-associated (*E. casseliflavus*, *E. mundtii*) *Enterococcus* species, and one group contained rare *Enterococcus* biotypes (“other” *Enterococcus*). Three additional non-enterococcal groups were also isolated. These organisms grow and produce enterococcus-like reactions on mEI agar (blue halo) but are not *Enterococcus*. These organisms were *Streptococcus bovis*, found in ruminant guts, *Aerococcus viridans*, and a group of unidentified non-enterococcal organisms collectively called the “not *Enterococcus*” group. During HB06, *E. casseliflavus* (~32%) was the dominant *Enterococcus* species observed, while *E. faecalis* (~22%) and *E. faecium* (~15%) were also common (SI Fig. 2). The dominance of *E. casseliflavus* during HB06 is notable, as *E. casseliflavus* is a plant- rather than fecal-associated species. Its dominance in the surfzone at Huntington Beach, and other nearby beaches (Ferguson et al., 2005; Moore et al., 2008), suggests that the use of total *Enterococcus* counts without subsequent species identification may lead to spurious identification of surfzone fecal pollution.

Statistically significant differences were observed in the *Enterococcus* species composition onshore vs. offshore (Chi-square  $p$ -value < 0.01). Onshore, *E. casseliflavus*, *E. faecalis* and *E. faecium* all occurred at high percentages (>17% each), while offshore, concentrations of *E. faecium* were only ~8%, reducing it from a major (onshore) to a minor (offshore) constituent. Furthermore, the percentage of *E. mundtii* was much higher offshore than onshore (14% vs. 7%), and *E. hirae*, *A. viridans*, rare *Enterococcus* biotypes, and non-enterococcal organisms were more prevalent offshore (Fig. 1). The differences in *Enterococcus* species composition across shore are consistent with the results of the hindcast model (Rippy et al., in press, their Fig. 3), which identified two sources of

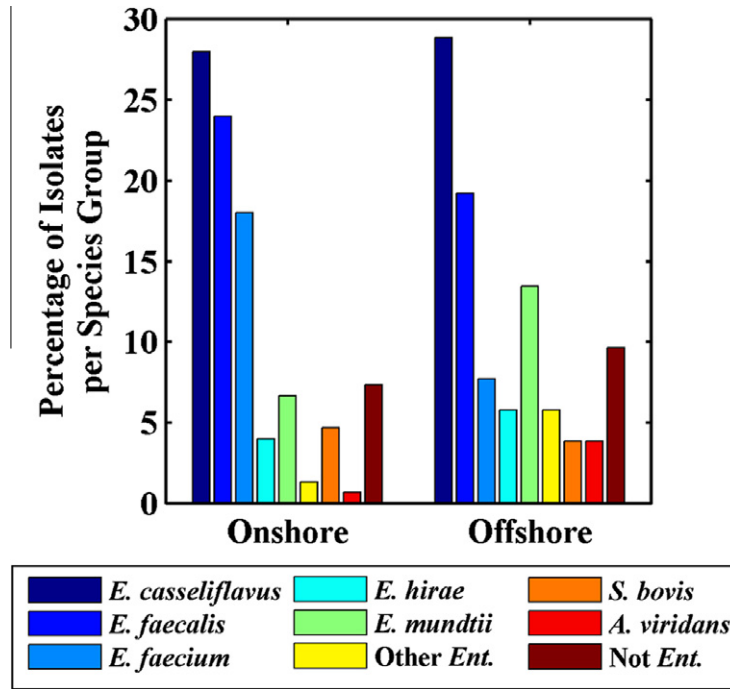


Fig. 1. Species composition of onshore (SAR, TM, FHM, and F1) vs. offshore (F5 and F7) HB06 *Enterococcus* isolates. Note that the percentage of *E. faecium* exceeds that of *E. mundtii* at onshore, but not offshore, stations.

*Enterococcus* (a northern onshore source and a southern offshore source) at Huntington Beach. These results also lend credence to the source-specific mortality formulations in the ADS and ADSI models, which parameterize the mortality of onshore and offshore FIB differently based on the assumption that FIB from different sources can have different exposure histories or species compositions, and thus different mortality rates (Sinton et al., 2002).

3.2. Solar insolation vs. decay

October 16th, 2006, was partially cloudy with maximum solar insolation levels of  $445 \text{ J m}^{-2} \text{ s}^{-1}$  measured at 13:00. No significant relationship was detected between solar insolation dose ( $\text{J m}^{-2}$ ,

integrated over the 20 min sampling interval) and *E. coli* decay rate at any station over the study period. Measured *Enterococcus* decay rates, however, increased significantly with solar insolation dose, but only at offshore stations (50–150 m offshore) (Fig. 2).

The general lack of correlation between solar insolation dose and FIB decay (especially for *E. coli*) was unexpected, as prior research has indicated a clear relationship between sunlight and FIB mortality in seawater (Boehm et al., 2005; Sinton et al., 2002; Troussellier et al., 1998). It is possible, however, that solar insolation did contribute to FIB decay at Huntington Beach, and that detection of this effect was obscured by the contribution of physical dilution (via advection and diffusion) to decay (Rippy et al., in press).

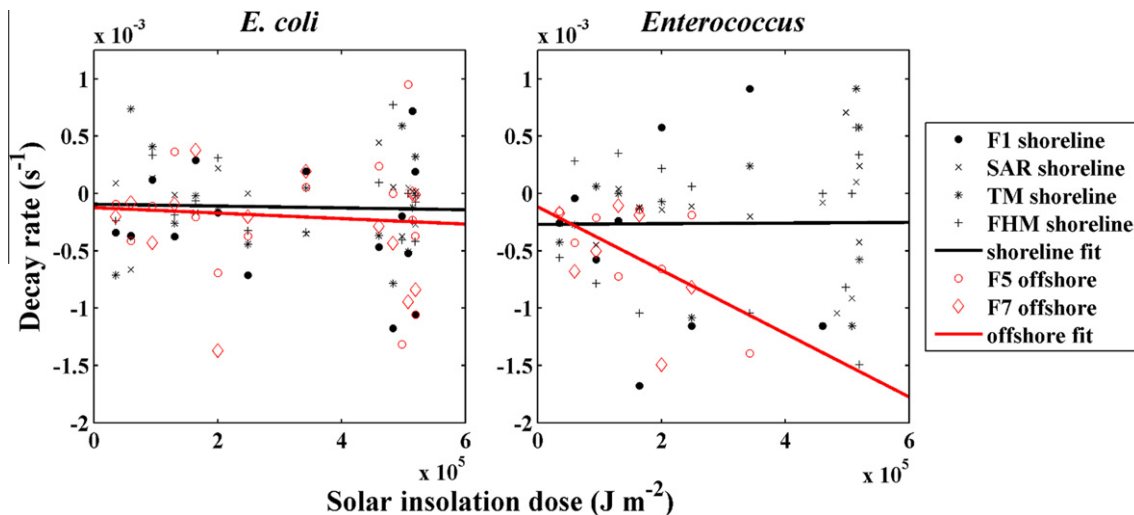


Fig. 2. *E. coli* and *Enterococcus* decay rate vs. solar insolation dose averaged over shoreline (black) and offshore (red) locations. The lines are best-fit slopes. The regression skill ( $R^2 = 0.22$ ) is significant ( $p < 0.05$ ) for offshore *Enterococcus*, but not for *E. coli* or shoreline *Enterococcus*.

**Table 1**  
Best-fit mortality parameters for FIB models.

		Model formulation							
		Mortality parameters ( $s^{-1}$ )	AD	ADC	ADI	ADS	ADG	ADSI	ADGI
<i>E. coli</i> models									
1 Parameter models	$m$	–	$7.5 \times 10^{-5}$	$1.2 \times 10^{-4}$	–	–	–	–	–
	Range of $m^*$	–	–	$6.1 \times 10^{-6}$ – $1.2 \times 10^{-4}$	–	–	–	–	–
2 Parameter models	$m_0^a$	–	–	–	$1.0 \times 10^{-6}$	$1.0 \times 10^{-6}$	$1.0 \times 10^{-6}$	$1.0 \times 10^{-6}$	$1.0 \times 10^{-6}$
	Range of $m_0^*$	–	–	–	–	–	$5.1 \times 10^{-8}$ – $1.0 \times 10^{-6}$	$5.1 \times 10^{-8}$ – $1.0 \times 10^{-6}$	$5.1 \times 10^{-8}$ – $1.0 \times 10^{-6}$
	$m_1^b$	–	–	–	$2.0 \times 10^{-4}$	$2.0 \times 10^{-4}$	$4.0 \times 10^{-4}$	$4.0 \times 10^{-4}$	$4.0 \times 10^{-4}$
	Range of $m_1^*$	–	–	–	–	–	$2.0 \times 10^{-5}$ – $4.0 \times 10^{-4}$	$2.0 \times 10^{-5}$ – $4.0 \times 10^{-4}$	$2.0 \times 10^{-5}$ – $4.0 \times 10^{-4}$
<i>Enterococcus</i> models									
1 Parameter models	$m$	–	$1.0 \times 10^{-4}$	$2.0 \times 10^{-4}$	–	–	–	–	–
	Range of $m^*$	–	–	$1.0 \times 10^{-5}$ – $2.0 \times 10^{-4}$	–	–	–	–	–
2 Parameter models	$m_0^a$	–	–	–	$1.6 \times 10^{-4}$	$1.0 \times 10^{-4}$	$2.5 \times 10^{-4}$	$2.0 \times 10^{-4}$	$2.0 \times 10^{-4}$
	Range of $m_0^*$	–	–	–	–	–	$1.3 \times 10^{-5}$ – $2.5 \times 10^{-4}$	$1.0 \times 10^{-5}$ – $2.0 \times 10^{-4}$	$1.0 \times 10^{-5}$ – $2.0 \times 10^{-4}$
	$m_1^b$	–	–	–	$4.0 \times 10^{-4}$	$4.0 \times 10^{-4}$	$2.0 \times 10^{-3}$	$1.5 \times 10^{-3}$	$1.5 \times 10^{-3}$
	Range of $m_1^*$	–	–	–	–	–	$1.0 \times 10^{-4}$ – $2.0 \times 10^{-3}$	$7.6 \times 10^{-4}$ – $1.5 \times 10^{-3}$	$7.6 \times 10^{-4}$ – $1.5 \times 10^{-3}$

\* Mortality ranges are only applicable for models where mortality is not constant in time (ADI, ADSI, and ADGI).

<sup>a</sup>  $m_0$  is the surfzone mortality parameter.

<sup>b</sup>  $m_1$  is the offshore mortality parameter.

The significant correlation found between solar insolation dose and FIB decay for offshore *Enterococcus* (Fig. 2) supports the role of solar insolation in regulating *Enterococcus* mortality seaward of the surfzone. This finding motivates testing insolation-dependent mortality models for this FIB group, particularly those that allow the relationship between solar insolation dose and FIB decay to vary across shore (ADSI and ADGI models).

### 3.3. Mortality models: best-fit parameter values

All mortality models were sensitive to the selection of mortality parameters:  $m$  for the one-parameter models (ADC and ADI) and  $m_0$  and  $m_1$  (surfzone and offshore mortality) for the two-parameter models (ADS, ADSI, ADG and ADGI) (SI Figs. 3–6). For all two-parameter mortality models, skill was more sensitive to changes in the offshore mortality parameter than the surfzone mortality parameter (SI Figs. 5 and 6). This indicates that mortality may be a dominant processes contributing to FIB decay offshore, where the influences of advection and diffusion are weaker (Rippey et al., in press).

Mortality parameters for *Enterococcus* were larger overall than those for *E. coli* for every model (Table 1). This is consistent with the slower overall decay observed for *E. coli* during the HB06 study (Rippey et al. in press). For the ADS, ADSI, ADG, and ADGI models, the offshore mortality parameter ( $m_1$ ) was always higher than the surfzone mortality parameter ( $m_0$ ) for both FIB groups (Table 1), indicating that cross-shore variable FIB mortality is needed to accurately reproduce observed FIB concentrations.

Best-fit mortality values for *E. coli* (all models) corresponded roughly to values reported for *E. coli* mortality in seawater ( $1.3 \times 10^{-6}$ – $8.1 \times 10^{-4} s^{-1}$ ) (Sinton et al., 2007; Troussellier et al., 1998) (Table 1). For all two-parameter *E. coli* models, offshore mortality rates were at the lower edge of reported mortality rate ranges, and surfzone mortality rates were at the upper edge (Sinton et al., 2007; Troussellier et al., 1998) (Table 1). Best-fit mortality values for *Enterococcus* (ADC, ADI, ADS and ADG) also corresponded roughly to reported *Enterococcus* mortality rates ( $4.4 \times 10^{-5}$ – $4.7 \times 10^{-4} s^{-1}$ ) (Boehm et al., 2005) (Table 1). Notably, maximum offshore *Enterococcus* mortality values for the ADSI and ADGI models (range:  $7.6 \times 10^{-5}$ – $2 \times 10^{-3}$ ) exceeded reported rates (Boehm et al., 2005) (Table 1).

### 3.4. Best-fit model-data comparisons: physical and physical-mortality models compared

The mortality models performed better than the AD model in reproducing FIB concentrations during HB06. The superior performance of the mortality models is most notable at offshore stations F5 and F7, where AD modeled FIB concentrations were too high (Figs. 3 and 4). Including mortality significantly improved model skill at these offshore stations, with skill estimates increasing from <0.05 (AD model) to >0.37 (Mortality models) for both FIB groups (Fig. 5). Model skill also improved at surfzone stations, but these improvements were smaller in magnitude (Fig. 5). This underscores the importance of mortality as a factor contributing to FIB decay in offshore waters.

### 3.5. Best-fit model-data comparisons: FIB mortality mechanisms

Although all forms of mortality improved model predictions, FIB concentrations (Figs. 3 and 4) and station-specific decay rates (Fig. 6) were most accurately reproduced by mortality functions with cross-shore dependence – either onshore/offshore sources (ADS, ADSI) or a persistent cross-shore mortality gradient (ADG, ADGI). This finding is consistent with the *Enterococcus* speciation and solar insolation dose results discussed above, which revealed differences in onshore vs. offshore *Enterococcus* species composition and response to solar insolation dose (Figs. 1 and 2).

It is notable, given the emphasis on solar-induced mortality in FIB literature (Boehm et al., 2005; Sinton et al., 2002; Troussellier et al., 1998), that mortality functions with cross-shore variability in mortality rates had higher skill than those including only time-dependent solar mortality. This is not to say that coastal FIB decay is not a function of solar insolation dose; the insolation-dependent ADGI and ADSI models performed extremely well for both *E. coli* and *Enterococcus* (Figs. 5 and 6). ADI performance, however, was significantly worse than either ADG or ADS, suggesting that the importance of time-dependent solar dose was secondary to the importance of cross-shore variability of mortality (Figs. 5 and 6).

No best-fit mortality model was identified for *Enterococcus* – all models with cross-shore variable FIB mortality (ADS, ADSI, ADG, and ADGI) had similar skill and predicted *Enterococcus* decay rates accurately ( $p < 0.05$ ) at the same number of sampling stations (6 of

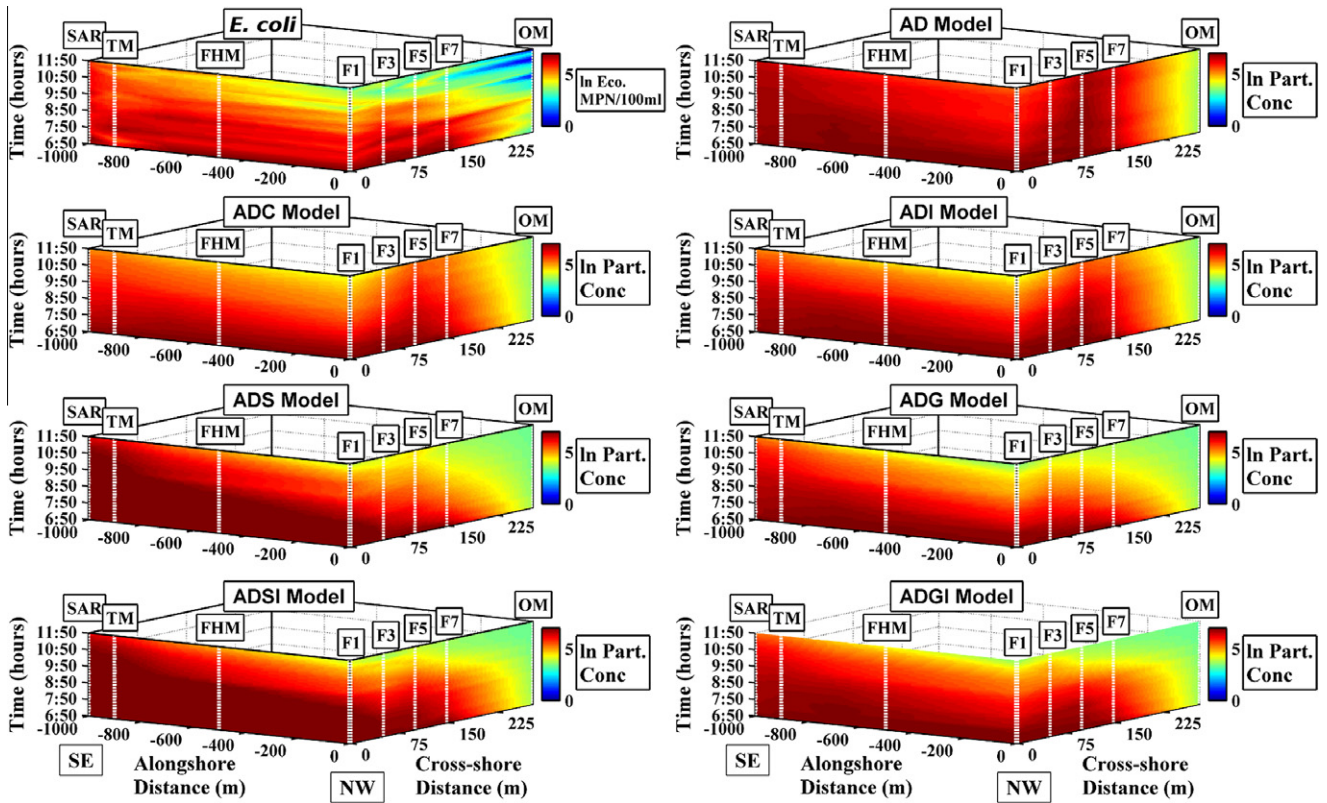


Fig. 3. Contour plots of *E. coli* data, and best-fit model outputs as a function of cross-shore distance (m), alongshore distance (m), and time (h). On the alongshore axis, the northernmost station (F1) is located at 0 m, with negative values indicating stations to the south. Color bar units are in natural log Most Probable Number (MPN) for *E. coli* data, and natural log of particle concentration for the mortality models. Note the over retention of *E. coli* particles at offshore stations with the AD, ADC, and ADI models.

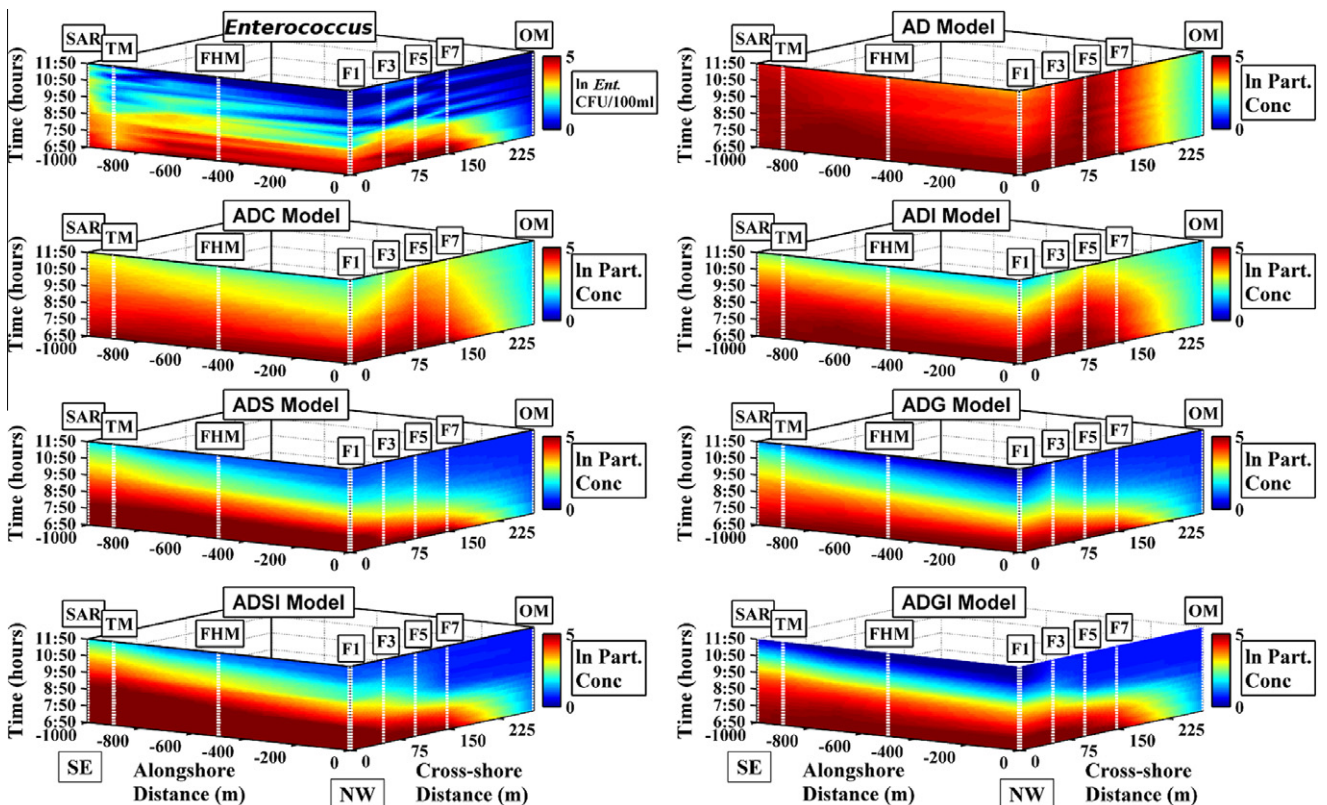
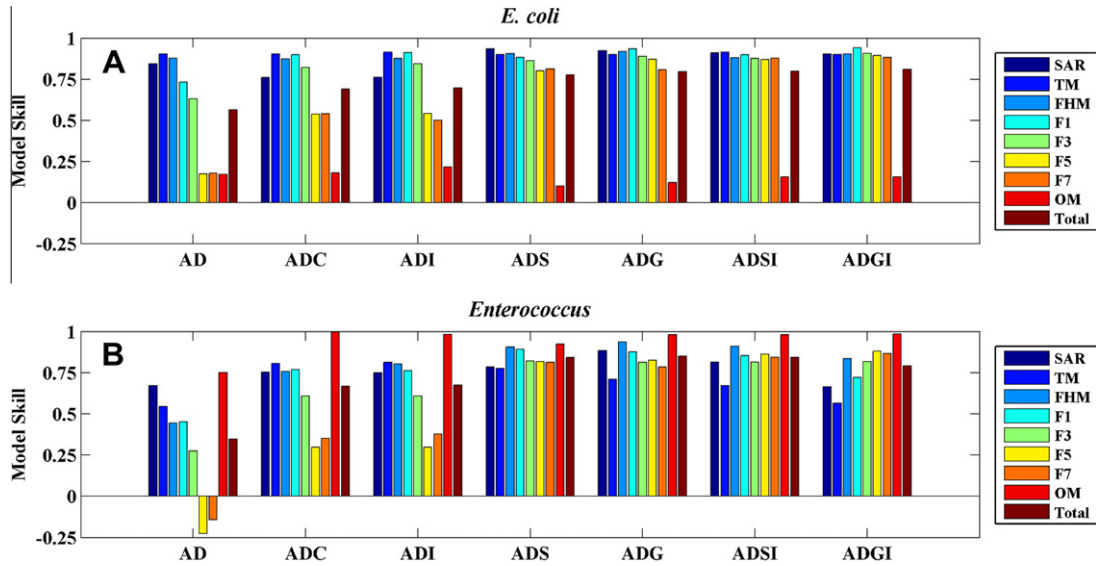
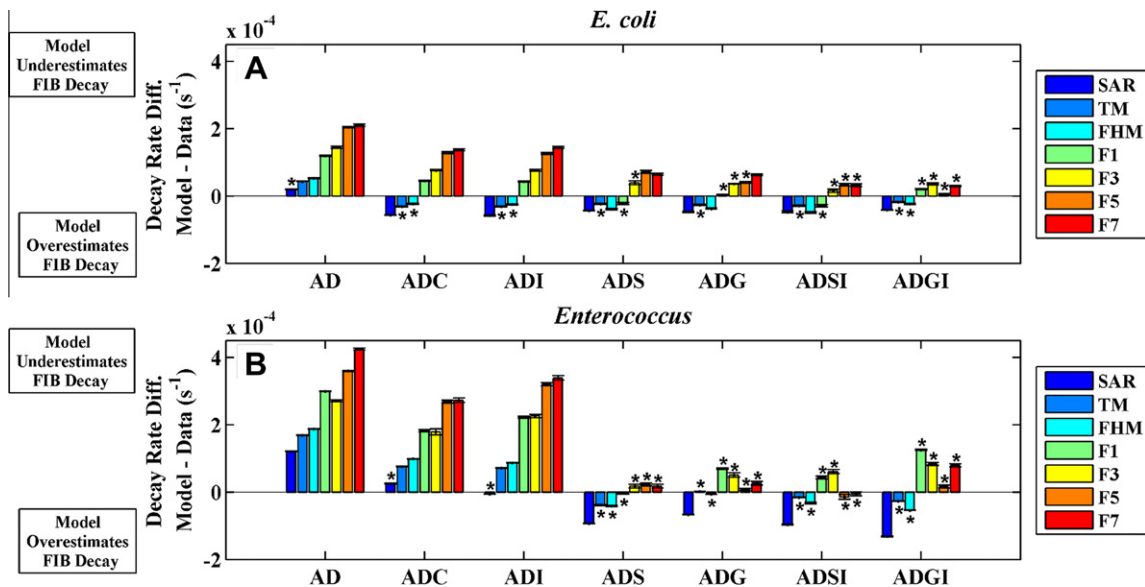


Fig. 4. Contour plots of *Enterococcus* data. Axes are the same as Fig. 3. Color bar units are in natural log Colony Forming Units (CFUs) for *Enterococcus* data, and natural log of particle concentration for the mortality models. Note the over retention of *Enterococcus* particles at offshore stations with the AD, ADC, and ADI models.



**Fig. 5.** Station-specific and total skill for best-fit *E.coli* (A) and *Enterococcus* (B) models, where total skill refers to a bulk estimate calculated across all sampling stations. All mortality models improve model skill relative to the AD model at each sampling station, for both FIB groups. Model skill is highest for the models allowing for cross-shore variable FIB mortality (ADS, ADG, ADSI, and ADGI).



**Fig. 6.** Decay rate differences (model – data) at each sampling station, for each best-fit model: (A) *E. coli* and (B) *Enterococcus*. An asterisk indicates decay rate differences that are not significantly different from zero ( $p < 0.05$ ).

7) (Figs. 5 and 6). For *E. coli*, cross-shore variable mortality models also had similar skill (Fig. 5). That said, the ADGI model (including both cross-shore variable and solar-induced mortality) performed slightly better than the other three, reproducing *E. coli* decay rates accurately ( $p < 0.05$ ) at the greatest number of sampling stations (6 of 7) (Fig. 6).

The superior performance of cross-shore variable mortality models for both FIB groups at Huntington Beach highlights the need for further research regarding the spatial variability of FIB mortality in nearshore systems. Our data were insufficient to distinguish among the various cross-shore variable FIB mortality hypotheses we explored, and thus the mechanisms underlying this variability remain unknown. Given the superior performance of the ADGI model for *E. coli*, however, special attention should be paid to processes that cause cross-shore gradients of insolation, such as

turbidity. Field-based microcosm experiments could be useful in this regard.

Based on the exponential FIB decay observed during our study our models focused on extra-enteric FIB mortality. FIB, however, have been reported to grow and/or undergo inactivation/repair cycles in aquatic systems (Boehm et al., 2009; Surbeck et al., 2010). For this reason our estimated mortality rates are better interpreted as net rates, including some unknown combination of mortality, inactivation, and growth. *E. coli*, for example, has been shown to exhibit elevated growth rates in highly turbulent flows (Al-Homoud and Hondzo, 2008). Thus one interpretation of our cross-shore variable net mortality rates for *E. coli* (low in the surfzone and higher offshore) could be a relatively constant baseline mortality rate with some level of additional growth (lower net mortality) in the surfzone. Similarly, it is possible that some

portion of the FIB loss we attribute to mortality (surfzone or off-shore) is instead inactivation due to photodamage, and that some of these damaged FIB could undergo repair and recover. This would make actual FIB mortality rates lower than those estimated from our models (Boehm et al., 2009). More extensive experiments, monitoring a broader range of biological parameters, are required to piece together the processes contributing to the patterns in net FIB mortality revealed by our Huntington Beach FIB models.

Although observed FIB decay has often been attributed to mortality alone, and can likewise be attributed to physical processes alone (e.g., the AD model), we have shown the importance of including both mortality and advection/diffusion in models predicting nearshore FIB concentrations. Furthermore, our study shows the importance of understanding the functional form of mortality, emphasizing that mortality can vary in both space and time. Because of this, accurate predictive FIB models are likely to be location-specific, with mortality functions reflecting dominant local FIB sources and/or spatial gradients in bacterial stressors. Our success at modeling short-term changes in FIB concentrations at Huntington Beach is encouraging, and further study (more extensive data sets, spanning longer time periods and spatial extents) is warranted to explore the effectiveness of individual based models for long-term FIB prediction.

### Acknowledgements

This work was partially funded by NSF, ONR, CA SeaGrant (NOAA project #NA10OAR4170060, California Sea Grant Project #25793B; through NOAA's National Sea Grant College Program, U.S. Dept. of Commerce), the California Coastal Conservancy, the California Department of Boating and Waterways Oceanography program, and NOAA. The statements, findings, conclusions and recommendations are those of the author(s) and do not necessarily reflect the views of the aforementioned organizations. Tests for FIB analysis were provided and performed by the Orange County Sanitation District and the Orange County Public Health Laboratory. Special thanks to volunteers from the Integrative Oceanography Division (B. Woodward, B. Boyd, D. Clark, K. Smith, D. Darnell, I. Nagy, J. Leichter, M. Omand, M. Yates, M. McKenna, S. Henderson, D. Michrokowski) for their assistance in data collection.

### Appendix A. Supplementary material

Supplementary data associated with this article can be found, in the online version, at <http://dx.doi.org/10.1016/j.marpolbul.2012.09.003>.

### References

- Al-Homoud, A., Hondzo, M., 2008. Enhanced uptake of dissolved oxygen and glucose by *Escherichia coli* in a turbulent flow. *Appl. Microbiol. Biotechnol.* 79, 643–655.
- Alkan, U., Elliot, D.J., Evison, L.M., 1995. Survival of enteric bacteria in relation to simulated solar radiation and other environmental factors in marine waters. *Water Res.* 29, 2071–2081.
- Boehm, A.B., Grant, S.B., Kim, J.H., Mowbray, S.L., McGee, C.D., Clark, C.D., Foley, D.M., Wellman, D.E., 2002. Decadal and shorter period variability of surf zone water quality at Huntington Beach, California. *Environ. Sci. Technol.* 36, 3885–3892.
- Boehm, A.B., 2003. Model of microbial transport and inactivation in the surf zone and application to field measurements of total coliform in northern Orange County, California. *Environ. Sci. Technol.* 37, 5511–5517.
- Boehm, A.B., Shellenbarger, G.G., Paytan, A., 2004. Groundwater discharge: potential association with fecal indicator bacteria in the surf zone. *Environ. Sci. Technol.* 38, 3558–3566.
- Boehm, A.B., Keymer, D.P., Shellenbarger, G.G., 2005. An analytical model of *enterococci* inactivation, grazing, and transport in the surf zone of a marine beach. *Water Res.* 39, 3565–3578.
- Boehm, A., Yamahara, K., Love, D.C., Peterson, B.M., McNeill, K., Nelson, K.L., 2009. Covariation and photoinactivation of traditional and novel indicator organisms and human viruses at a sewage-impacted marine beach. *Environ. Sci. Technol.* 43, 8046–8052.
- Curtis, T.P., Mara, D.D., Silva, S., 1992. Influence of pH, oxygen, and humic substances on ability of sunlight to damage fecal coliforms in waste stabilization pond water. *Appl. Environ. Microbiol.* 58, 1335–1343.
- Ferguson, D.M., Moore, D.F., Getrich, M.A., Zhou, M.H., 2005. Enumeration and speciation of *enterococci* found in marine and intertidal sediments and coastal water in southern California. *J. Appl. Microbiol.* 99, 598–608.
- Gersberg, R.M., Rose, A.M., Robles-Sikisaka, R., Dhar, A.K., 2006. Quantitative detection of hepatitis A virus and enteroviruses near the United States–Mexico border and correlation with levels of fecal indicator bacteria. *Appl. Environ. Microbiol.* 72, 7438–7444.
- Grant, S.B., Sanders, B.F., Boehm, A.B., Redman, J.A., Kim, J.H., Mrse, R.D., Chu, A.K., Gouldin, M., McGee, C.D., Gardiner, N.A., Jones, B.H., Svejksky, J., Leipzig, G.V., Brown, A., 2001. Generation of *enterococci* bacteria in a coastal saltwater marsh and its impact on surf zone water quality. *Environ. Sci. Technol.* 35, 2407–2414.
- Hartke, A., Giard, J., Laplace, J., Auffray, Y., 1998. Survival of *Enterococcus faecalis* in an oligotrophic microcosm: changes in morphology, development of general stress resistance, and analysis of protein synthesis. *Appl. Environ. Microbiol.* 64, 4238–4245.
- Hartke, A., Lemarinier, S., Pichereau, V., Auffray, Y., 2002. Survival of *Enterococcus faecalis* in seawater microcosms is limited in the presence of bacterivorous zooflagellates. *Curr. Microbiol.* 44, 329–335.
- Krause, P., Boyle, D.P., Base, F., 2005. Comparison of different efficiency criteria for hydrological model assessment. *Adv. Geosci.* 5, 89–97.
- Moore, D.F., Guzman, J.A., McGee, C., 2008. Species distribution and antimicrobial resistance of *enterococci* isolated from surface and ocean water. *J. Appl. Microbiol.* 105, 1017–1025.
- Omand, M.M., Leichter, J.J., Franks, P.J.S., Guza, R.T., Lucas, A.J., Feddersen, F., 2011. Physical and biological processes underlying the sudden surface appearance of a red tide in the nearshore. *Limnol. Oceanogr.* 56, 787–801.
- Reniers, A.J.H.M., MacMahan, J.H., Thornton, E.B., Stanton, T.P., Henriquez, M., Brown, J.W., Brown, J.A., Gallagher, E., 2009. Surf zone surface retention on a rip-channel beach. *J. Geophys. Res.* 114, C10010–C10022.
- Rippey, M.A., Franks, P.J.S., Feddersen, F., Guza, R.T., Moore, D.F., in press. Physical dynamics controlling variability in nearshore fecal pollution: Fecal Indicator Bacteria as passive particles. *Mar. Pollut. Bull.* <http://dx.doi.org/10.1016/j.marpolbul.2012.09.030>.
- Sanders, B.F., Arega, F., Sutula, M., 2005. Modeling the dry-weather tidal cycling of fecal indicator bacteria in surface waters of an intertidal wetland. *Water Res.* 39, 3394–3408.
- Sinton, L.W., Hall, C.H., Lynch, P.A., Davies-Colley, R.J., 2002. Sunlight inactivation of fecal indicator bacteria and bacteriophages from waste stabilization pond effluent in fresh and saline waters. *Appl. Environ. Microbiol.* 68, 1122–1131.
- Sinton, L., Hall, C., Braithwaite, R., 2007. Sunlight inactivation of *Campylobacter jejuni* and *Salmonella enterica*, compared with *Escherichia coli*, in seawater and river water. *J. Water Health.* 5, 357–365.
- Smith, J.A., Largier, L., 1995. Observations of nearshore circulation: rip currents. *J. Geophys. Res.* 100, C10967–C10975.
- Solic, M., Krstulovic, N., 1992. Separate and combined effects of solar radiation, temperature, salinity, and pH in the survival of fecal coliforms in seawater. *Mar. Pollut. Bull.* 24, 411–416.
- Surbeck, C.Q., Jiang, S.C., Grant, S.B., 2010. Ecological control of fecal indicator bacteria in an urban stream. *Environ. Sci. Technol.* 44, 631–637.
- Troussellier, M., Bonnefont, J., Courties, C., Derrien, A., Dupray, E., Gauthier, M., Gourmelon, M., Joux, F., Lebaron, P., Martin, Y., Pommepuy, M., 1998. Responses of enteric bacteria to environmental stresses in seawater. *Oceanol. Acta* 21, 965–981.
- Whitman, R.L., Nevers, M.B., Korinek, G.C., Byappanahalli, M.N., 2004. Solar and temporal effects on *Escherichia coli* concentration at a Lake Michigan swimming beach. *Appl. Environ. Microbiol.* 70, 4276–4285.
- Yamahara, K.M., Layton, B.A., Santoro, A.E., Boehm, A.B., 2007. Beach sands along the California coast are diffuse sources of fecal bacteria to coastal waters. *Environ. Sci. Technol.* 41, 4515–4521.